

Discrete Prior-Based Temporal-Coherent Content Prediction for Blind Face Video Restoration

Lianxin Xie¹, Bingbing Zheng¹, Wen Xue¹, Yunfei Zhang¹, Le Jiang¹, Ruotao Xu², Si Wu^{1,2*},
Hau-San Wong^{3*}

¹School of Computer Science and Engineering, South China University of Technology

²Institute of Super Robotics(Huangpu)

³Department of Computer Science, City University of Hong Kong

{cslianxin.xie, 202321044369, csxuewen, cszhangyunfei, csjiangle}@mail.scut.edu.cn
rtxu@superbots.com, cswusi@scut.edu.cn, cshswong@cityu.edu.hk

Abstract

Blind face video restoration aims to restore high-fidelity details from videos subjected to complex and unknown degradations. This task poses a significant challenge of managing temporal heterogeneity while at the same time maintaining stable face attributes. In this paper, we introduce a Discrete Prior-based Temporal-Coherent content prediction transformer to address the challenge, and our model is referred to as DP-TempCoh. Specifically, we incorporate a spatial-temporal-aware content prediction module to synthesize high-quality content from discrete visual priors, conditioned on degraded video tokens. To further enhance the temporal coherence of the predicted content, a motion statistics modulation module is designed to adjust the content, based on discrete motion priors in terms of cross-frame mean and variance. As a result, the statistics of the predicted content can match with that of real videos over time. By performing extensive experiments, we verify the effectiveness of the design elements and demonstrate the superior performance of our DP-TempCoh in both synthetically and naturally degraded video restoration. Code is available at <https://github.com/lxxie298/DP-TempCoh>.

Introduction

The task of blind face video restoration(BFVR) aims to restore high-quality face image sequences from degraded videos, and the main challenge is to address various unknown degradations while at the same time preserving the dynamic consistency of the synthesized content. The degraded face videos typically exhibit temporal heterogeneity. Even if the frames of a face video are subjected to similar degradations, each restored face may appear different from the others significantly. As shown in Figure 1, state-of-the-art blind face restoration and video restoration methods, DiffBIR and FMA-Net, fail to synthesize faces with stable characteristics.

To synthesize clear and realistic face images from degraded ones, a number of image enhancement methods incorporate various face priors into the generation process,

* Corresponding authors.



Figure 1: An example to visually compare the proposed DP-TempCoh with the competing image/video restoration methods: DiffBIR and FMA-Net, in restoration quality and temporal coherence.

such as high-quality (HQ) reference samples with the same identity or geometric information(Li et al. 2018)(Dogan, Gu, and Timofte 2019). On the other hand, the well-trained Generative Adversarial Networks (GANs)(Chen et al. 2016) on high-quality face datasets has the capability of generating diverse and realistic face images, and thus there are attempts to apply the pre-trained generator as generative priors to face image enhancement(Zhu et al. 2022)(Wang et al. 2021)(Wang, Hu, and Zhang 2022)(Menon et al. 2020). On the other hand, Stable Diffusion(Rombach et al. 2021) has also exhibited impressive generation ability in face image generation recently (Lin et al. 2023)(Wang et al. 2023)(Kim

et al. 2022)(Zhao et al. 2023). Since the GAN- and diffusion-based methods are designed for processing images, directly applying them to face video restoration inevitably results in the synthesized results with unexpected temporal discontinuities. There are also methods that attempted to improve the temporal consistency of diffusion model, in which they fine-tuned diffusion model by adding temporal block including 3D convolution(Wang et al. 2024)(Blattmann et al. 2023) and temporal attention(Chen et al. 2023)(Zhou et al. 2022a). Although these modifications enhance video stability, the inherent randomness of diffusion sampling can still lead to significant variations between reconstructed sequences.

In this paper, we present a Discrete Prior-based Temporal-Coherent content prediction transformer (DP-TempCoh) for high-fidelity blind face video restoration. Specifically, the proposed DP-TempCoh mainly consists of a visual prior-based spatial-temporal-aware content prediction module and a motion prior-based statistics modulation module. To deal with the temporal heterogeneity issues in BFVR task and enhance the content consistency of the restored video, the content prediction module learns to generate the features of high-quality content from discrete visual priors in terms of latent bank, conditioned on the contextual information of degraded video frames. Further, the modulation module is incorporated to enhance the temporal coherence by modulating the predicted content, based on the motion priors in terms of cross-frame mean and variance. We have performed extensive experiments to verify the effectiveness of the designed modules and demonstrate the superior performance of our DP-TempCoh in real-world face video restoration with unknown degradation. The main contributions of this work are summarized as follows:

- We propose a novel blind face video restoration framework to synthesize high-fidelity and temporal-coherent content by leveraging two types of complementary discrete priors.
- We transform the spatial-temporal features of degraded video tokens by matching with the discrete visual priors in terms of a latent bank learnt from external high-quality face videos.
- To improve the temporal coherence of synthesized face videos, we construct discrete motion priors in terms of cross-frame mean and variance, and perform modulation on the transformed video token features, such that the resulting ones can match with the temporal statistics of real face videos.

Related Work

Video Enhancement

An important video enhancement task is super-resolution, which aims to restore high-resolution (HR) video frame sequences from degraded low resolution (LR) video frames while preserving the original semantics. Due to the fact that adjacent frames in video sequences can provide reference information to each other, there are a number of temporal sliding-window based VSR methods that processed LR frames in a time sliding window manner. STTN(Kim et al.

2018) selectively warped target frames for enhancement using the estimated optical flow. (Liu et al. 2017) proposed a spatial alignment network for neighboring frames alignment. Another line of research involves utilizing recurrent neural networks to harness temporal information from multiple frames. RLSP(Fuoli, Gu, and Timofte 2019) propagated high-dimensional hidden states to better capture long-term information. BasicVSR(Chan et al. 2021) utilized a recurrent network design with bidirectional propagation to enhance video quality and detail by leveraging information from neighboring frames. BasicVSR++(Chan et al. 2022) built upon this framework by adding a second-stage refinement network and alignment module to further improve the precision and stability of the super-resolution process. Nevertheless, these methods have not incorporated suitable generative priors, which made them struggle to restore content that has lost texture details. Recently, diffusion-based methods have made great progress(Esser et al. 2023)(Hu, Chen, and Luo 2023)(Ho et al. 2022). Upscale-A-Video(Zhou et al. 2024a) proposed text-guided latent diffusion framework for video enhancement, in which a flow-guided recurrent latent propagation module was used to enhance temporal stability. However, in BVFR task, it is difficult for the model to obtain stable optical flow from degraded data, which could negatively affect the performance of the restoration model.

Blind Face Restoration

Significant progress has been achieved in face image restoration in recent years. There are methods that introduced facial landmarks (Hu et al. 2021; Lin et al. 2020), face parsing maps(Chen et al. 2021), or 3D shapes(Zhu et al. 2022) in their designs. However, prior information obtained from degraded images often contains significant noise, which could lead to a performance drop. On the other hand, a number of recent works focus on exploring how to utilize the generative priors in generative models, such as StyleGAN2(Karras et al. 2020), Stable Diffusion(Rombach et al. 2021), etc, to assist in image restoration. GFP-GAN(Wang et al. 2021) and GPEN (Yang et al. 2021) leveraged facial spatial features to guide the restoration model, enabling it to utilize the geometric and texture priors of the pretrained StyleGAN. However, these methods overly relied on the facial features of degraded images, which made them sensitive to facial noise. To handle degradations robustly, DR2(Wang et al. 2023) added Gaussian noise to the degraded images, and then restored them through a pre-trained diffusion model to achieve the effect of removing degradation. DiffBIR(Lin et al. 2023) first removed degradation without generating new content, and then restored face details based on a pre-trained Stable Diffusion model(Rombach et al. 2021). However, because these methods were specifically designed for the task of image restoration and involve randomness in sampling, they could result in issues such as discontinuity and flickering when applied to sequences of degraded face images. There are also methods that attempted to utilize sparse representation with learned dictionaries to address image restoration tasks which took advantage of dictionary information in different ways to represent degraded images(Gu et al. 2022; Wang et al. 2022; Zhou et al. 2022b). Re-

storeFormer learned fully-spatial interactions between corrupted queries and high-quality dictionary key-value pairs, and CodeFormer built a code sequences prediction module to exploit the dictionary information. However, these methods were specifically designed for image restoration, and did not take into account temporal coherence in the video restoration task.

Different from the above dictionary-based methods, we model visual priors with respect to videos, capture the inter-relationships among video tokens, and predict high-quality token features from the priors to replace the degraded ones. In addition, we perform cross-frame statistics modulation with motion priors, such that the predicted content can be further improved in terms of temporal coherence. This design distinguishes the proposed approach from the existing face restoration and video enhancement methods.

Proposed Method

Overview

We introduce a novel BFVR method of applying visual prior-based content prediction to restore degraded features, and leveraging motion prior-based statistics modulation to enhance temporal coherence. The structure of our framework is depicted in Figure 2 and comprises four main components: an Encoder E , a Visual Prior-based Spatial-temporal-aware Content Prediction Module C , a Motion Prior-based Statistics Modulation module M , and a Generator G . The process begins with the Encoder E , which transforms frames from degraded video clips v_{lq} into a sequence of video tokens. These tokens z are then processed by the content prediction module C , which generate the features z' of high-quality content from a vision bank. Features z' is further refined by the motion prior-based statistic modulation Module M , which adjusts the cross-frame mean and variance of z' , resulting in a motion-enhanced representation z'' . Subsequently, several cross-attention-based transformer were applied to merge z' and z'' , forming the feature \hat{z} that corresponds to a high-quality and temporally smooth face video. The feature \hat{z} are then decoded by G to reconstruct the face video clip \hat{v} that aims to achieve maximum consistency with the ground truth. This reconstruction process contributes to the fidelity and fluidity of the restored video.

Spatial-temporal-aware Content Prediction

Traditional image restoration techniques typically focus on individual frames, thus neglecting the dynamic inter-dependencies among successive frames, which makes it difficult to fully utilize the spatial information between frames in the video clip, especially for degraded video. To address this problem, the proposed spatial-temporal-aware content prediction module, conditioned on degraded video tokens, predicts index values from the pre-trained vision bank \mathbb{T} . The vision bank is constructed through vector quantization during the high-quality image reconstruction process, in which each index corresponds to a high-quality visual representation. In order to effectively predict index values \hat{l} with nuanced contextual associations, we model both the spatial and temporal information of degraded video clips. Initially,

video clip tokens z , extracted from encoder E , are flattened. To enhance the model’s capability of interpreting spatial and temporal positioning of each token, we integrate a learnable spatial-temporal position embedding into each token. Subsequently, multiple self-attention-based transformer blocks, coupled with an activation function, calculate the likelihood of each token belonging to a particular bank’s index. The process of index prediction can be formalized as follows:

$$\tilde{z} = \xi'(\text{SA}(\xi(z) + \mathbf{P}_{emb})), \quad (1)$$

$$\hat{l}_{i,j,k} = \arg \max_{r \in \{0,1,\dots,N\}} \psi(\tilde{z}_{i,j,k})_r, \quad (2)$$

where \mathbf{P}_{emb} represents the learnable spatial-temporal position embedding, ξ and ξ' denote the flatten and unflatten operations respectively, SA denotes the self-attention based transformer, $\psi(\cdot)_r$ denotes the softmax activation output on r -th index and $\hat{l}_{i,j,k} \in \{0, 1, \dots, N\}$ denotes the predicted index of bank, where N is the size of the bank \mathbb{T} , and i, j , and k represent the spatial and temporal locations of the video clip tokens. By computing the index l , we can match the corresponding features of high-quality content in the bank as follows:

$$z'_{i,j,k} = \kappa(\mathbb{T}, \hat{l}_{i,j,k}), \quad (3)$$

where κ represents using an index $\hat{l}_{i,j,k}$ to extract features from the bank \mathbb{T} and z' denotes the high quality face features. The self-attention-based computation facilitates the modeling of the relationships between tokens across multiple frames, such that the module can predict index values by extracting complementary information from different tokens, eventually combining the extracted features to create a representation of high-quality content with contextual association and dynamic consistency.

Motion Prior-based Statistics Modulation

In order to further enhance the temporal coherence of the predicted content, we introduce the motion prior-based statistics modulation module. Initially, we construct a statistics bank, denoted as \mathbb{M} , which is trained using high-quality face videos. The bank \mathbb{M} is designed to store the cross-frame mean and variance vectors whose components are the channel mean and variance corresponding to each frame. During the processing of features z' , we first calculate the mean and variance in the channel dimension for each frame as follow:

$$\mu_{f,w,h} = \sum_c \frac{z'_{f,c,h,w}}{L_C}, \quad (4)$$

$$\sigma_{f,w,h}^2 = \frac{\sum_c (z'_{f,c,h,w} - \mu_{f,w,h})^2}{L_C}, \quad (5)$$

where L_C denotes the channel size of z' . Subsequently, we concatenate $\mu_{f,w,h}$ and $\sigma_{f,w,h}^2$ in the temporal dimension to generate a mean vector and a variance vector, respectively. The mean and variance vectors are then concatenated, and a nearest matching algorithm is employed to retrieve the corresponding element from \mathbb{M} , which can be formalized as follows:

$$[\mu'_{w,h}, \sigma'^2_{w,h}] = \arg \min_{e \in \mathbb{M}} \|\text{Concat}(\mu_{w,h}, \sigma_{w,h}^2) - e\|_2^2, \quad (6)$$

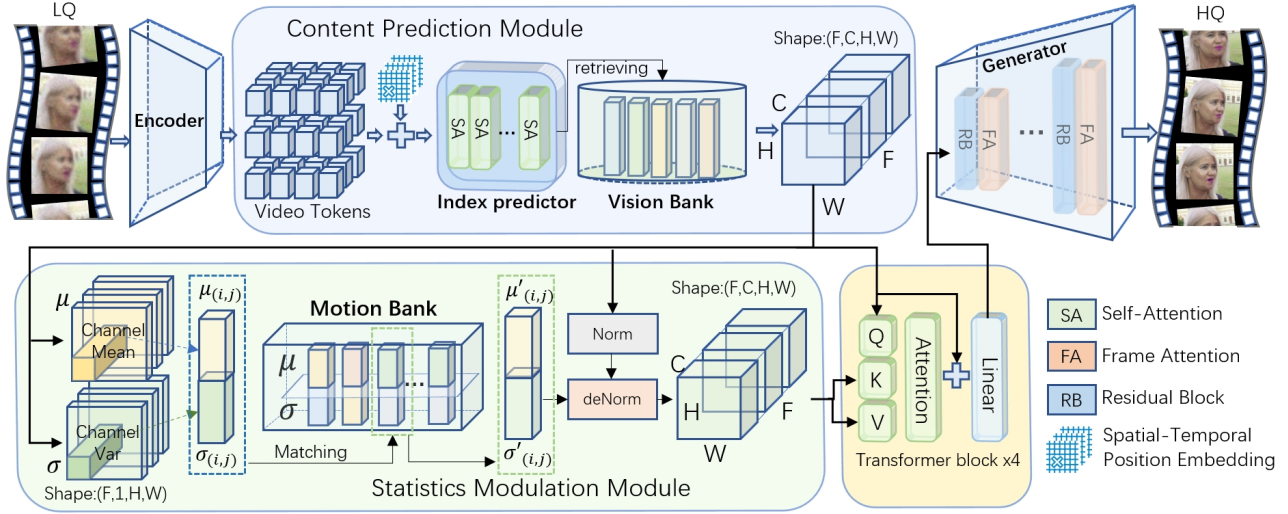


Figure 2: Overview of the proposed DP-TempCoh framework. An encoder E extracts the tokens z from a degraded face video segment v_{lq} . A latent spatial-temporal-aware content prediction module is applied to z to predict z' that enriched spatial and temporal contextual information. Next, a prior-based motion statistics modulation module modulates the statistics of z' to obtain z'' . We perform several cross-attention-based transformer computation over z' and z'' , and feed the resulting feature into a generator G to synthesize a HQ face video \hat{z} .

where Concat represents the concatenation operation in the temporal dimension. We exploit the mean $\mu'_{w,h}$ and variance $\sigma'^2_{w,h}$ vectors with high-quality motion priors to modulate predicted content z' , as follows:

$$z''_{f,w,h} = \sigma'_{f,w,h} \frac{z'_{f,w,h} - \mu'_{f,w,h}}{\sigma'_{f,w,h} + \epsilon} + \mu'_{f,w,h}, \quad (7)$$

where ϵ is a small real value and $z''_{f,w,h}$ denotes the modulated feature. The modulation of mean and variance is tailored to maintain temporal coherence of predicted content, thereby mitigating issues like flickering. In addition, we incorporate a cross-attention based transformer block, in which feature z' serves as the query and z'' is used as both the key and value. This arrangement allows for a comprehensive integration of content information with modulated features, which can be formalized as follows:

$$\hat{z} = \xi'(\text{CA}(\xi(z'), \xi(z''))), \quad (8)$$

where $\text{CA}(a, b)$ denotes the transformer block in which a, b denote query and key-value input, respectively. We restore the clear face video clip \hat{v} by inputting \hat{z} into the generator G . The transformer block is optimized together with G . To enhance the temporal coherence of restored texture, we have integrated multiple 3D residual blocks and frame attention mechanisms into G .

Model Training

Let \hat{v} denote the restored face video clip derived from a degraded input v_{lq} . Initially, we employ pixel-level loss to ensure consistency with the ground truth, defined as:

$$\mathcal{L}_{consi} = \mathbb{E}_{(v, v_{hq})} [|\hat{v} - v_{hq}|_1 + |\phi(\hat{v}) - \phi(v_{hq})|_1], \quad (9)$$

where v_{hq} denotes the ground-truth high quality video clip with respect to v_{lq} , and ϕ represents the feature maps extracted by a pre-trained VGG19 (Simonyan and Zisserman 2014). For the purpose of improving the visual quality of restored video segments, We also adopt an adversarial training loss as follows:

$$\begin{aligned} \mathcal{L}_{adv}^{real} &= \mathbb{E}_{v_{hq}} [\log D(v_{hq})], \\ \mathcal{L}_{adv}^{sync} &= \mathbb{E}_{v_{lq}} [\log(1 - D(\hat{v}))], \end{aligned} \quad (10)$$

where $D(\cdot)$ denotes the predicted probability of an input face image being real. In addition, we employ a cross entropy loss to train the spatial-temporal-aware content prediction module as follows:

$$\mathcal{L}_{bank} = \mathbb{E}_{v_{lq}} \left[- \sum_{i,j,k} z_{i,j,k}^{gt} \log(\psi(\tilde{z}_{i,j,k})) \right], \quad (11)$$

where ψ represents the softmax activation function and z^{gt} denotes the ground truth of bank index labels which is derived from the pre-trained encoder E and vision bank \mathbb{T} . By integrating the above training losses, we formulate the optimization problem of our restoration model as follows:

$$\begin{aligned} \min_{E,C,G} \quad & \mathcal{L}_{consi} + \mathcal{L}_{adv}^{sync} + \lambda \mathcal{L}_{bank}, \\ \max_D \quad & \mathcal{L}_{adv}^{real} + \mathcal{L}_{adv}^{sync}, \end{aligned} \quad (12)$$

where λ denotes a weighting factor that controls the relative importance of content prediction term.

Experiments

In this section, we conduct extensive experiments to evaluate the proposed DP-TempCoh on a wide range of blind face

video restoration tasks. Initially, we outline the experimental settings, which include descriptions of the training and test datasets, implementation details, and evaluation protocol. Subsequently, we comprehensively investigate the effectiveness of the prior-based modules in face video restoration. This is followed by quantitative and qualitative comparisons with state-of-the-art methods.

Experimental Settings

Training Data DP-TempCoh was trained on VFHQ(Xie et al. 2022), which is a high-quality video face dataset and contains over 15,000 high-fidelity clips of diverse interview scenarios. To construct LQ training face videos, we follow(Yang et al. 2021) to degrade the VFHQ video frames as follows:

$$v_{lq}^f = ((v_{hq}^f \otimes \mathcal{K}_{\rho'}) \downarrow_{b'} + n_{\sigma'})_{JPEG_{w'}}, \quad (13)$$

where $v_{lq/hq}^f$ denotes f -th frame in video clip $v_{lq/hq}$. Each HQ frame is first convolved with the Gaussian blur kernel which has a standard deviation $\rho' \in [\rho - 1, \rho + 1]$ where $\rho \in \{1 : 0.1 : 10\}$. Afterwards, it is downsampled $b' \in [b - 1, b + 1]$ times where $b \in \{2 : 32\}$, and is corrupted by Gaussian noise with intensity parameter $\sigma' \in [\sigma - 1, \sigma + 1]$ where $\sigma \in \{0 : 10\}$. Furthermore, the JPEG compression with quality factor $w' \in [w - 5, w + 5]$ where $w \in \{50 : 100\}$ is then applied to the resulting frames.

Test Data We assess the restoration performance of the proposed DP-TempCoh and the competing methods on three benchmark datasets: HDTF(Zhang et al. 2021), VFHQ-Test(Xie et al. 2022) and YouTube Faces dataset(Wolf, Hassner, and Maoz 2011). HDTF includes about 16 hours of high-resolution videos and VFHQ-Test has 100 video clips. We randomly sample clips from each video and apply the degradation operation defined in Eq.13 to construct degraded video clips, and the resulting test dataset is referred to as HDTF-Deg and VFHQ-Test-Deg. In addition, YTF-Medium/Hard are derived from the YouTube Faces, and there are 500/520 in-the-wild face video clips with medium/heavy degradations.

Implementation Details We implement the model using PyTorch on two NVIDIA A800s. For optimization, we use the Adam (Kingma and Ba 2014) algorithm with a learning rate of 8×10^{-5} . The training process spans 200,000 iterations with a batch size of 4. The weighting factor λ in Eq.12 is set to 0.5. The sizes of the vision and motion banks are 1,024 and 16,384, respectively. The size of each video clip processed by the model is 8 frames.

Evaluation Protocol We implement all the competing methods based on the open source codes. The widely used metrics, Peak Signal-to-Noise Ratio (PSNR), Learned Perceptual Image Patch Similarity (LPIPS) and the Fréchet Inception Distances (FID) (Heusel et al. 2017), are used to quantitatively evaluate the restored videos. We additionally report the IDentity Similarity (IDS) based on a well-trained face recognition model: CosFace (Wang et al. 2018). Considering the temporal coherency is critical for BVFR, we

further report the inter-frame difference (IFD) which evaluates video coherency by calculating the pixel mean square error between consecutive frames.

Content Prediction

In this section, we assess the effectiveness of our content prediction module. First of all, we analyze the convergence of this module. To illustrate the role of spatial-temporal context in accelerating convergence speed, we replace spatial-temporal-aware content prediction module (labeled as ‘S & T-aware’) with spatial-aware version (labeled as ‘S-aware’) which do not consider the relationship between frames. As

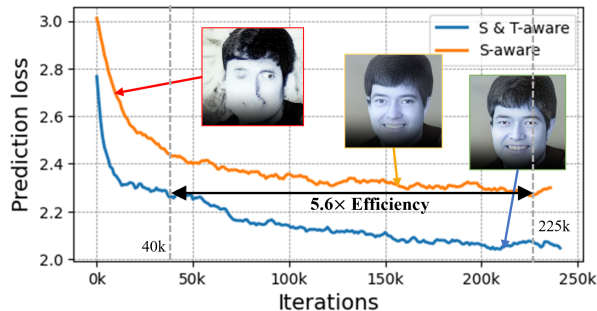


Figure 3: Convergence comparison between spatial-temporal-aware (S & T-aware) and spatial-aware (S-aware) prediction loss.



Figure 4: Visualization of stable attention maps corresponding to the query of left eye.

shown in Figure 3, at the beginning of training, distortions are noticeable in the restored face. When converging to the same position, ‘S-aware’ requires 5.6 times more iterations than ‘S & T-aware’. After convergence, both methods can restore face semantics well, but ‘S & T-aware’ has better facial details. To ascertain whether the module leverages contextual information of degraded video frames, we visualize the attention maps of the last transformer block in Figure 4. The region of left eye serves as query, and the four attention maps on the right hand side show the responses corresponding to the query. It is worth noting that the module exhibits a heightened focus on the left eye region across different poses. The result suggests that our model effectively captures contextual information from multiple frames to restore the content on the current position.

Ablation Study

Does prior-based spatial-temporal prediction aid restoration? To verify the efficacy of the proposed

Exp	Module			Metrics		
	S-aware	S & T-aware	Motion	PSNR \uparrow	FID \downarrow	IFD \downarrow
(a)	✓			23.12	72.14	9.86
(b)		✓		24.52	55.11	3.92
(c)			✓	12.55	210.12	5.59
(d)		✓	✓	25.12	52.04	3.80

Table 1: Results of ablative models on VFHQ-Test-Deg. ‘S-aware’, ‘S & T-aware’ and ‘Motion’ denote spatial-aware prediction, spatial-temporal-aware prediction and motion statistics modulation module, respectively.

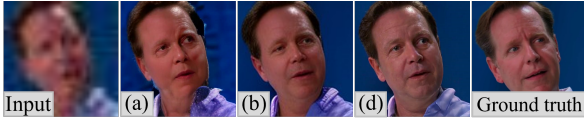


Figure 5: Visual comparison between DP-TempCoh and ablative models(defined in Table 1) on VFHQ-Test-Deg video.

spatial-temporal-aware content prediction module, we conducted a comparative experiment between (a) and (b) where (a) is equipped with a spatial-aware (labeled as ‘S-aware’) content prediction module which does not have token information exchange between frames and (b) used the proposed spatial-temporal-aware component (labeled as ‘S & T-aware’). As shown in Table 1, when using ‘S-aware’, all performance metrics decrease compared to the ‘S & T-aware’ version, e.g., the PSNR is reduced by 1.4. This decline can be attributed to the model’s inability to account for the spatial and temporal context across multiple frames. Additionally, as depicted in Figure 5, the quality of facial restoration was slightly compromised.

Can motion prior-based statistics modulation improve temporal coherence? We initially assess if statistics modulation enhances temporal feature coherence in latent space by comparing average Euclidean distances between consecutive frames. To verify whether the modulation module can improve the temporal coherence in the video space, we replaced the S-aware module in (a) with the statistics modulation module and named it (c). As shown in Table 1, it can be seen that while the FID score increased and PSNR score decreased, IFD score decreased from 9.86 to 3.92. In experiment (d), we introduced the statistics modulation module based on experiment (b), which led to a reduction in the IFD score from 3.92 to 3.80. At the same time, both PSNR and FID metrics showed improvements. As shown in figure 5, it can be observed that both qualitative and quantitative comparisons show improvements in (d), indicating that adding the statistics modulation module to the content prediction module can further enhance the quality and temporal coherence of restored videos.

Comparison to State-of-the-arts

To demonstrate the superiority of the proposed DP-TempCoh, we perform quantitative and qualitative compar-

isons with state-of-the-arts, including the following image enhancement methods: CodeFormer(Zhou et al. 2022b), RestoreFormer(Wang et al. 2022), DR2(Wang et al. 2023), DiffBIR(Lin et al. 2023), DiffFace(Yue and Loy 2024), and video enhancement methods: BasicVSR++(Chan et al. 2022), MIA-VSR(Zhou et al. 2024b), IA-RT(Xu et al. 2024), FMA-Net(Youk, Oh, and Kim 2024).

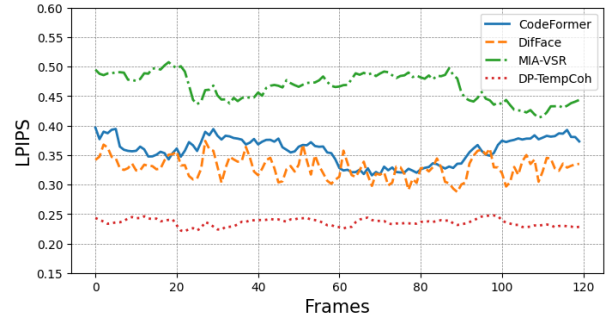


Figure 6: Comparison of DP-TempCoh and competing methods in terms of restoration stability.

Results on synthetic data We conducted a comparative experiment in which DP-TempCoh and competing methods were used to restore degraded face videos. The results of the methods are summarized in Table 2. CodeFormer and DiffFace achieve lower FID and LPIPS values than the other competing methods, which indicates that they perform better in terms of the precision and realism of the restored face sequences. In addition, the competing video restoration methods can achieve lower IFD value, suggesting that they can restore a coherent sequence of face images. On the other hand, DP-TempCoh surpasses the competing methods in terms of all the metrics. In particular, DP-TempCoh is able to achieve the highest IDS score, which reflects that it faithfully preserves the identity. In addition, DP-TempCoh achieves the IFD and FID scores of 3.13 and 25.65, which are lower than the second best methods (BasicVSR++ IDF 5.21; CodeFormer: FID 34.14) by 2.08 and 8.49, respectively. To verify whether the proposed DP-TempCoh can achieve more coherent face image sequence restoration, Figure 6 presents the LPIPS metric of the proposed method and the competing methods across a sequence of video frames. The diffusion-based method, DiffFace, shows notable fluctuations in metric LPIPS, indicating instability. Although both CodeFormer and MIA-VSR exhibit less variability, it underperform in terms of the LPIPS metric. In contrast, our proposed method consistently excels in terms of LPIPS scores and maintains stable performance across all frames.

Results on in-the-wild data To verify the generalization ability of the proposed model, we further assess DP-TempCoh and competing methods on YTF-Medium/Hard. As shown in Table 2, the DP-TempCoh model not only attains IDF metrics comparable to those of existing video restoration methods but also achieves the best FID values. The representative results shown in Figure 7 demonstrate the

Methods	VFHQ-Test-Deg					HDTF-Deg					YTF-Medium		TYF-Hard	
	PSNR \uparrow	IDS \uparrow	LPIPS \downarrow	FID \downarrow	IFD \downarrow	PSNR \uparrow	IDS \uparrow	LPIPS \downarrow	FID \downarrow	IFD \downarrow	FID \downarrow	IFD \downarrow	FID \downarrow	IFD \downarrow
Image Restoration Methods														
CodeFormer (Zhou et al. 2022b)	24.75	0.7115	0.3562	65.68	9.86	24.55	0.7323	0.3254	34.14	8.64	65.15	7.6	72.25	9.86
RestoreFormer (Wang et al. 2022)	23.54	0.6034	0.4737	95.25	10.42	23.37	0.6543	0.4529	52.62	11.26	72.82	8.12	81.12	10.31
DR2 (Wang et al. 2023)	22.28	0.5411	0.4109	87.57	10.46	23.55	0.5916	0.3586	37.67	8.38	76.51	9.60	79.02	11.47
DiffBIR (Lin et al. 2023)	23.96	0.6826	0.3643	66.85	11.91	23.09	0.6464	0.3488	41.25	12.35	69.74	10.21	80.18	13.42
DiffFace (Yue and Loy 2024)	25.01	0.6526	0.3483	63.73	9.82	24.63	0.6341	0.3281	34.47	8.75	68.12	11.10	83.34	11.48
Video Restoration Methods														
BasicVSR++ (Chan et al. 2022)	24.84	0.4802	0.4573	189.10	5.11	24.45	0.4851	0.4618	210.36	5.21	92.86	5.55	120.54	7.40
MIA-VSR (Zhou et al. 2024b)	24.77	0.4756	0.5163	168.12	5.44	24.38	0.4816	0.5219	125.68	5.24	132.07	6.05	185.93	7.44
IA-RT (Xu et al. 2024)	24.78	0.4754	0.5165	171.65	5.43	24.38	0.4814	0.5223	128.83	5.25	128.15	6.06	182.67	7.54
FMA-Net (Youk, Oh, and Kim 2024)	24.73	0.4464	0.4914	179.94	6.99	24.35	0.4515	0.4958	115.07	6.89	127.02	6.79	137.91	7.43
DP-TempCoh	25.12	0.7721	0.2262	52.04	3.80	24.71	0.7685	0.2427	25.65	3.13	51.86	5.51	55.50	7.38

Table 2: Quantitative Comparison between DP-TempCoh and competing methods on synthetic/in-the-wild data.

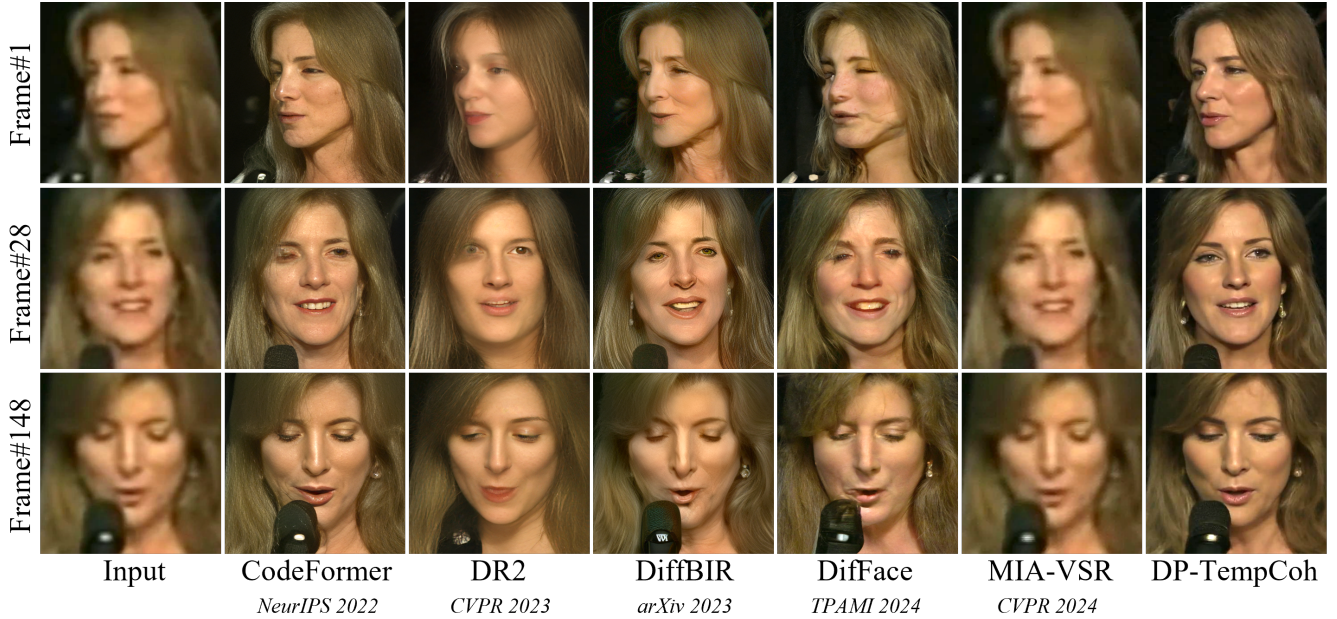


Figure 7: Visual comparison between DP-TempCoh and the competing methods on representative frames of in-the-wild videos.

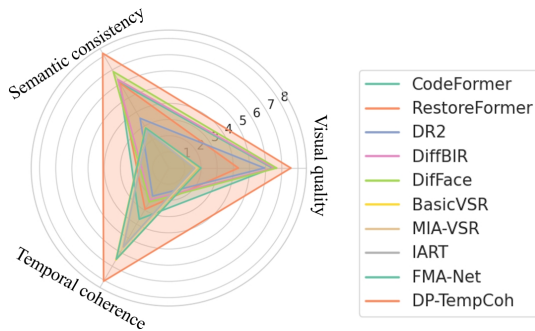


Figure 8: The scoring result of user study on wild data.

advantages of DP-TempCoh in reducing artifacts, restoring realistic details, and preserving dynamic consistency.

User Study We conduct a user study to evaluate the quality of restoration from three perspectives: visual qual-

ity, semantic consistency and temporal coherence. We randomly select 30 degraded face video clips from YTF-Medium/Hard, and enlist 30 workers to grade the restored video from above three perspectives on a scale from 0 to 10. High scores on visual quality, semantic consistency and temporal coherence indicate realistic details, high semantic similarity with the input image and coherent video content, respectively. Figure 8 displays three average scores achieved by each model. DP-TempCoh achieves the highest average scores in terms of three perspectives.

Conclusion

This paper presents a discrete prior-based temporal-coherent content prediction transformer to achieve high-quality face video restoration. We model the contextual information of degraded video frames to learn the interrelationships between frames, which allows us to effectively predict high-quality content from discrete visual priors. We further leverage the motion priors in terms of cross-frame mean and vari-

ance to modulate predicted content, which is essential for improving the temporal coherence of the restored video sequences. Comprehensive experimental results demonstrate that our content prediction and modulation modules can effectively generate high-quality content with dynamic consistency. A possible following up work is to apply our idea to diverse video restoration tasks, where the emergence of textual and visual prompts is concerned.

References

- Blattmann, A.; Rombach, R.; Ling, H.; Dockhorn, T.; Kim, S. W.; Fidler, S.; and Kreis, K. 2023. Align your latents: High-resolution video synthesis with latent diffusion models. In *Proceedings of the IEEE/CVF Conference on Computer Vision and Pattern Recognition*, 22563–22575.
- Chan, K. C.; Wang, X.; Yu, K.; Dong, C.; and Loy, C. C. 2021. Basicvsr: The search for essential components in video super-resolution and beyond. In *Proceedings of the IEEE/CVF conference on computer vision and pattern recognition*, 4947–4956.
- Chan, K. C.; Zhou, S.; Xu, X.; and Loy, C. C. 2022. Basicvsr++: Improving video super-resolution with enhanced propagation and alignment. In *Proceedings of the IEEE/CVF conference on computer vision and pattern recognition*, 5972–5981.
- Chen, C.; Li, X.; Yang, L.; Lin, X.; Zhang, L.; and Wong, K.-Y. K. 2021. Progressive semantic-aware style transformation for blind face restoration. In *Proceedings of the IEEE/CVF conference on computer vision and pattern recognition*, 11896–11905.
- Chen, H.; Xia, M.; He, Y.; Zhang, Y.; Cun, X.; Yang, S.; Xing, J.; Liu, Y.; Chen, Q.; Wang, X.; et al. 2023. Videocrafter1: Open diffusion models for high-quality video generation. *arXiv preprint arXiv:2310.19512*.
- Chen, X.; Duan, Y.; Houthoofd, R.; Schulman, J.; Sutskever, I.; and Abbeel, P. 2016. InfoGAN: interpretable representation learning by information maximizing generative adversarial nets. In *Proc. Neural Information Processing Systems*.
- Dogan, B.; Gu, S.; and Timofte, R. 2019. Exemplar guided face image super-resolution without facial landmarks. In *Proceedings of the IEEE/CVF conference on computer vision and pattern recognition workshops*, 0–0.
- Esser, P.; Chiu, J.; Atighehchian, P.; Granskog, J.; and Germanidis, A. 2023. Structure and content-guided video synthesis with diffusion models. In *Proceedings of the IEEE/CVF International Conference on Computer Vision*, 7346–7356.
- Fuoli, D.; Gu, S.; and Timofte, R. 2019. Efficient video super-resolution through recurrent latent space propagation. In *2019 IEEE/CVF International Conference on Computer Vision Workshop (ICCVW)*, 3476–3485. IEEE.
- Gu, Y.; Wang, X.; Xie, L.; Dong, C.; Li, G.; Shan, Y.; and Cheng, M.-M. 2022. Vqfr: Blind face restoration with vector-quantized dictionary and parallel decoder. In *European Conference on Computer Vision*, 126–143. Springer.
- Heusel, M.; Ramsauer, H.; Unterthiner, T.; Nessler, B.; and Hochreiter, S. 2017. Gans trained by a two time-scale update rule converge to a local nash equilibrium. *Advances in neural information processing systems*, 30.
- Ho, J.; Salimans, T.; Gritsenko, A.; Chan, W.; Norouzi, M.; and Fleet, D. J. 2022. Video diffusion models. *Advances in Neural Information Processing Systems*, 35: 8633–8646.
- Hu, X.; Ren, W.; Yang, J.; Cao, X.; Wipf, D.; Menze, B.; Tong, X.; and Zha, H. 2021. Face restoration via plug-and-play 3D facial priors. *IEEE Transactions on Pattern Analysis and Machine Intelligence*, 44(12): 8910–8926.
- Hu, Y.; Chen, Z.; and Luo, C. 2023. Lamd: Latent motion diffusion for video generation. *arXiv preprint arXiv:2304.11603*.
- Karras, T.; Laine, S.; Aittala, M.; Hellsten, J.; Lehtinen, J.; and Aila, T. 2020. Analyzing and improving the image quality of stylegan. In *Proceedings of the IEEE/CVF conference on computer vision and pattern recognition*, 8110–8119.
- Kim, K.; Kim, Y.; Cho, S.; Seo, J.; Nam, J.; Lee, K.; Kim, S.; and Lee, K. 2022. Diffface: Diffusion-based face swapping with facial guidance. *arXiv preprint arXiv:2212.13344*.
- Kim, T. H.; Sajjadi, M. S.; Hirsch, M.; and Scholkopf, B. 2018. Spatio-temporal transformer network for video restoration. In *Proceedings of the European conference on computer vision (ECCV)*, 106–122.
- Kingma, D. P.; and Ba, J. 2014. Adam: A method for stochastic optimization. *arXiv preprint arXiv:1412.6980*.
- Li, X.; Liu, M.; Ye, Y.; Zuo, W.; Lin, L.; and Yang, R. 2018. Learning warped guidance for blind face restoration. In *Proceedings of the European conference on computer vision (ECCV)*, 272–289.
- Lin, S.; Zhang, J.; Pan, J.; Liu, Y.; Wang, Y.; Chen, J.; and Ren, J. 2020. Learning to deblur face images via sketch synthesis. In *Proceedings of the AAAI Conference on Artificial Intelligence*, 11523–11530.
- Lin, X.; He, J.; Chen, Z.; Lyu, Z.; Fei, B.; Dai, B.; Ouyang, W.; Qiao, Y.; and Dong, C. 2023. Diffbir: Towards blind image restoration with generative diffusion prior. *arXiv preprint arXiv:2308.15070*.
- Liu, D.; Wang, Z.; Fan, Y.; Liu, X.; Wang, Z.; Chang, S.; and Huang, T. 2017. Robust video super-resolution with learned temporal dynamics. In *Proceedings of the IEEE International Conference on Computer Vision*, 2507–2515.
- Menon, S.; Damian, A.; Hu, S.; Ravi, N.; and Rudin, C. 2020. Pulse: Self-supervised photo upsampling via latent space exploration of generative models. In *Proceedings of the IEEE/CVF conference on computer vision and pattern recognition*, 2437–2445.
- Rombach, R.; Blattmann, A.; Lorenz, D.; Esser, P.; and Ommer, B. 2021. High-Resolution Image Synthesis with Latent Diffusion Models. *arXiv:2112.10752*.
- Simonyan, K.; and Zisserman, A. 2014. Very deep convolutional networks for large-scale image recognition. *arXiv preprint arXiv:1409.1556*.
- Wang, H.; Wang, Y.; Zhou, Z.; Ji, X.; Gong, D.; Zhou, J.; Li, Z.; and Liu, W. 2018. CosFace: Large Margin Cosine Loss

- for Deep Face Recognition. In *2018 IEEE/CVF Conference on Computer Vision and Pattern Recognition*, 5265–5274.
- Wang, X.; Li, Y.; Zhang, H.; and Shan, Y. 2021. Towards Real-World Blind Face Restoration with Generative Facial Prior. In *2021 IEEE/CVF Conference on Computer Vision and Pattern Recognition (CVPR)*, 9164–9174.
- Wang, X.; Yuan, H.; Zhang, S.; Chen, D.; Wang, J.; Zhang, Y.; Shen, Y.; Zhao, D.; and Zhou, J. 2024. Videocomposer: Compositional video synthesis with motion controllability. *Advances in Neural Information Processing Systems*, 36.
- Wang, Y.; Hu, Y.; and Zhang, J. 2022. Panini-Net: GAN prior based degradation-aware feature interpolation for face restoration. In *Proceedings of the AAAI Conference on Artificial Intelligence*, 2576–2584.
- Wang, Z.; Zhang, J.; Chen, R.; Wang, W.; and Luo, P. 2022. Restoreformer: High-quality blind face restoration from undegraded key-value pairs. In *Proceedings of the IEEE/CVF conference on computer vision and pattern recognition*, 17512–17521.
- Wang, Z.; Zhang, Z.; Zhang, X.; Zheng, H.; Zhou, M.; Zhang, Y.; and Wang, Y. 2023. Dr2: Diffusion-based robust degradation remover for blind face restoration. In *Proceedings of the IEEE/CVF Conference on Computer Vision and Pattern Recognition*, 1704–1713.
- Wolf, L.; Hassner, T.; and Maoz, I. 2011. Face recognition in unconstrained videos with matched background similarity. In *CVPR 2011*, 529–534. IEEE.
- Xie, L.; Wang, X.; Zhang, H.; Dong, C.; and Shan, Y. 2022. Vfhq: A high-quality dataset and benchmark for video face super-resolution. In *Proceedings of the IEEE/CVF Conference on Computer Vision and Pattern Recognition*, 657–666.
- Xu, K.; Yu, Z.; Wang, X.; Mi, M. B.; and Yao, A. 2024. Enhancing Video Super-Resolution via Implicit Resampling-based Alignment. In *Proceedings of the IEEE/CVF Conference on Computer Vision and Pattern Recognition*, 2546–2555.
- Yang, T.; Ren, P.; Xie, X.; and Zhang, L. 2021. Gan prior embedded network for blind face restoration in the wild. In *Proceedings of the IEEE/CVF conference on computer vision and pattern recognition*, 672–681.
- Youk, G.; Oh, J.; and Kim, M. 2024. FMA-Net: Flow-Guided Dynamic Filtering and Iterative Feature Refinement with Multi-Attention for Joint Video Super-Resolution and Deblurring. In *Proceedings of the IEEE/CVF Conference on Computer Vision and Pattern Recognition*, 44–55.
- Yue, Z.; and Loy, C. C. 2024. Difface: Blind face restoration with diffused error contraction. *IEEE Transactions on Pattern Analysis and Machine Intelligence*.
- Zhang, Z.; Li, L.; Ding, Y.; and Fan, C. 2021. Flow-guided one-shot talking face generation with a high-resolution audio-visual dataset. In *Proceedings of the IEEE/CVF Conference on Computer Vision and Pattern Recognition*, 3661–3670.
- Zhao, Y.; Hou, T.; Su, Y.-C.; Jia, X.; Li, Y.; and Grundmann, M. 2023. Towards authentic face restoration with iterative diffusion models and beyond. In *Proceedings of the IEEE/CVF International Conference on Computer Vision*, 7312–7322.
- Zhou, D.; Wang, W.; Yan, H.; Lv, W.; Zhu, Y.; and Feng, J. 2022a. Magicvideo: Efficient video generation with latent diffusion models. *arXiv preprint arXiv:2211.11018*.
- Zhou, S.; Chan, K.; Li, C.; and Loy, C. C. 2022b. Towards robust blind face restoration with codebook lookup transformer. *Advances in Neural Information Processing Systems*, 35: 30599–30611.
- Zhou, S.; Yang, P.; Wang, J.; Luo, Y.; and Loy, C. C. 2024a. Upscale-A-Video: Temporal-Consistent Diffusion Model for Real-World Video Super-Resolution. In *Proceedings of the IEEE/CVF Conference on Computer Vision and Pattern Recognition*, 2535–2545.
- Zhou, X.; Zhang, L.; Zhao, X.; Wang, K.; Li, L.; and Gu, S. 2024b. Video Super-Resolution Transformer with Masked Inter&Intra-Frame Attention. In *Proceedings of the IEEE/CVF Conference on Computer Vision and Pattern Recognition*, 25399–25408.
- Zhu, F.; Zhu, J.; Chu, W.; Zhang, X.; Ji, X.; Wang, C.; and Tai, Y. 2022. Blind face restoration via integrating face shape and generative priors. In *Proceedings of the IEEE/CVF conference on computer vision and pattern recognition*, 7662–7671.